THE JOURNAL OF BIOLOGICAL CHEMISTRY VOL. 291, NO. 20, pp. 10867–10875, May 13, 2016
© 2016 by The American Society for Biochemistry and Molecular Biology, Inc. Published in the U.S.A.

The Nuclear Receptor Rev-erbα Regulates Adipose Tissue-specific FGF21 Signaling*

Received for publication, February 1, 2016, and in revised form, March 16, 2016 Published, JBC Papers in Press, March 21, 2016, DOI 10.1074/jbc.M116.719120

Jennifer Jager[‡1], Fenfen Wang[‡1], Bin Fang[‡], Hee-Woong Lim[‡], Lindsey C. Peed[‡], David J. Steger[‡], Kyoung-Jae Won[‡], Alexei Kharitonenkov[§], Andrew C. Adams[¶], and Mitchell A. Lazar[‡2]

From the [‡]Division of Endocrinology, Diabetes, and Metabolism, Departments of Medicine and Genetics, and Institute for Diabetes, Obesity, and Metabolism, Perelman School of Medicine, University of Pennsylvania, Philadelphia, Pennsylvania 19104, the [§]Department of Chemistry, Indiana University Bloomington, Bloomington, Indiana 47405, and the [¶]Lilly Research Laboratories, Lilly Corporate Center, Indianapolis, Indiana 46285

FGF21 is an atypical member of the FGF family that functions as a hormone to regulate carbohydrate and lipid metabolism. Here we demonstrate that the actions of FGF21 in mouse adipose tissue, but not in liver, are modulated by the nuclear receptor Rev-erbα, a potent transcriptional repressor. Interrogation of genes induced in the absence of Rev-erbα for Rev-erbα-binding sites identified βKlotho, an essential coreceptor for FGF21, as a direct target gene of Rev-erbα in white adipose tissue but not liver. Rev-erbα ablation led to the robust elevated expression of βKlotho. Consequently, the effects of FGF21 were markedly enhanced in the white adipose tissue of mice lacking Rev-erbα. A major Rev-erbα-controlled enhancer at the *Klb* locus was also bound by the adipocytic transcription factor peroxisome proliferator-activated receptor (PPAR) γ, which regulates its activity in the opposite direction. These findings establish Rev-erbα as a specific modulator of FGF21 signaling in adipose tissue.

Adipose tissue is an important fat storage and endocrine organ whose dysfunction is closely associated with the development of obesity, diabetes mellitus, and cardiovascular disease (1–5). Nuclear receptors are DNA-binding proteins that directly regulate gene expression in response to ligands derived from endocrine glands, metabolism, diet, and the environment (6). They are widely believed to act as key regulators in various physiological processes, such as circadian rhythm, development, reproduction, energy homeostasis, and metabolism (7, 8).

The nuclear receptor Rev-erbα differs from other members of the nuclear receptor superfamily because it lacks a classical activation domain and thus functions as a constitutive repressor of transcription (9–11). Acting in this repressive manner, Rev-erbα has been described as a core component of the mammalian biological clock (12) that links circadian rhythms to metabolism in diverse tissues. Indeed, studies from different groups have revealed Rev-erbα as a key regulator of multiple biological processes in various metabolic tissues, including liver (13–15), macrophages (16), muscle (17), brown fat (18), and brain (19). However, little is known about potential role in white adipose tissue (WAT).[3]

FGF21 is an atypical member of the FGF superfamily that, because of a lack of a heparin binding domain, is able to escape into the circulation, functioning as a hormone to regulate carbohydrate and lipid metabolism (20, 21). In the metabolic context, FGF21 was first discovered to induce glucose uptake in 3T3L1 adipocytes (22). Subsequently it was demonstrated that FGF21 administration to obese rodents and non-human primates improves hyperglycemia, lowers elevated triglyceride levels, and reduces body weight (22–25). In rodents, the mechanisms underlying FGF21 actions include improving whole-body insulin sensitivity and β cell function, reducing hepatic lipogenesis, and enhancing brown fat thermogenic activity (22, 23, 25–27). These effects identify FGF21 as an attractive therapeutic agent for the treatment of metabolic disease. Mechanistically, FGF21 interacts directly with the extracellular domain of the membrane bound co-factor βKlotho (KLB) in the FGF21-KLB-FGF receptor (FGFR) complex to activate FGF receptor substrate 2α and ERK1/2 phosphorylation (28–30). Although FGFRs are expressed in most tissues, KLB expression is restricted to a few, including liver, WAT, brown adipose tissue (BAT), and hypothalamus (31). Mice lacking KLB are resistant to both acute and chronic effects of FGF21. However, the acute insulin-sensitizing effects of FGF21 are also absent in mice with specific deletion of adipose KLB (32) or FGFR1 (33), consistent with the notion that direct adipose tissue activation is required for FGF21 action (34).

Here, based on integrated analysis of transcriptomes and cistromes in Rev-erbα KO mice, we found that KLB mRNA and

* This work was supported by National Institutes of Health Grants R01 DK45586 and DK49780, and the JPB Foundation. M. A. L. is a consultant to Lilly, A. K. is a former employee of Lilly, and A. C. A. is a current employee of Lilly. The content is solely the responsibility of the authors and does not necessarily represent the official views of the National Institutes of Health.
The microarray data and ChIP-seq reported in this paper have been submitted to the Gene Expression Omnibus Repository with accession number GSE79166.
The GRO-seq data reported in this paper have been submitted to the Gene Expression Omnibus Repository with accession number GSE79168.
[1] Both authors contributed equally to this work.
[2] To whom correspondence should be addressed: Division of Endocrinology, Diabetes, and Metabolism, Depts. of Medicine and Genetics, and Institute for Diabetes, Obesity, and Metabolism, Perelman School of Medicine, University of Pennsylvania, 12–102 Smilow Center for Translational Research, 3400 Civic Center Blvd., Philadelphia, PA 19104. Tel.: 215-898-0198; Fax: 215-898-5408; E-mail: lazar@mail.med.upenn.edu.

[3] The abbreviations used are: WAT, white adipose tissue; PPAR, peroxisome proliferator-activated receptor; KLB, βKlotho; FGFR, FGF receptor; BAT, brown adipose tissue; ZT, zeitgeber time; EWAT, epididymal white adipose tissue; ChIP-seq, ChIP sequencing; GRO-seq, global run-on sequencing; IWAT, inguinal white adipose tissue; eRNA, enhancer RNA; RT-qPCR, quantitative real-time PCR.

protein are markedly induced in WAT, but not in BAT or liver, of mice lacking Rev-erbα. Moreover, mice lacking Rev-erbα were hyperresponsive to FGF21 in WAT. These results reveal a tissue-specific modulation of FGF21 signaling by Rev-erbα via the repression of βKlotho.

Experimental Procedures

Animals—The Rev-erbα KO mice were obtained from B. Vennström and backcrossed for more than seven generations with C57/Bl6 mice. They were maintained on a standard diet under 12 h-light/12 h-dark cycles. The experiments were performed on 12- to 15-week-old males and females. The tissues were harvested at zeitgeber time (ZT) 10 (5 p.m.) when Rev-erbα protein level peaks in WT mice. Recombinant human FGF21 was provided by Lilly Research Laboratories. Animal care and use procedures followed the guidelines of the Institutional Animal Care and Use Committee of the University of Pennsylvania in accordance with the guidelines of the National Institutes of Health.

Reverse Transcription and Quantitative Real-time PCR (RT-qPCR)—Total RNA was isolated from tissues using TRIzol (Invitrogen), followed by purification with the RNEasy mini kit (Qiagen). 1 μg of purified RNA was used to generate cDNA (Applied Biosystems), and RT-qPCR analysis was performed. Amplicons were detected with Power SYBR Green Master Mix (Applied Biosystems). Relative gene expression levels were determined by the standard curve method, followed by normalization to the housekeeping gene 36B4.

Microarray—Each RNA sample was processed with the Ambion WT expression kit and the GeneChip WT terminal labeling and controls kit (Affymetrix), and hybridized to the Mouse Gene 1.0 ST Array (Affymetrix). Differential gene expression was determined using a one-way analysis of variance with cutoff of a *p* value of 0.05/0.01 and a -fold change of 1.3/1.5. The EWAT microarray data are available in the GEO under accession number GSE79166. The microarray data of PPARγ knockdown in 3T3-L1 adipocytes are from GEO accession number GSE14004 (35).

Immunoblotting—Primary antibodies for mouse βKlotho (R&D Systems, catalog no. AF2619, goat antibody), mouse Rev-erbα (Cell Signaling Technology, catalog no. CS2124, rabbit antibody), and mouse HSP90 (Santa Cruz Biotechnology, catalog no. sc-101494, mouse antibody) were detected by secondary horseradish peroxidase-conjugated antibodies (Sigma) and an enhanced chemiluminescent substrate kit (Perkin Elmer Life Sciences, Western Lightning).

ChIP—Mice were euthanized, and tissue was harvested immediately, quickly minced, and cross-linked in 1% formaldehyde for 20 min, followed by quenching with 1/20 volume of 2.5 M glycine solution and two washes with PBS. Cell lysates with fragmented chromatin were prepared by probe sonication in ChIP dilution buffer (50 mM HEPES, 155 mM NaCl, 1.1% Triton X-100, 0.11% sodium deoxycholate, 0.1% SDS, 1 mM PMSF, and a complete protease inhibitor tablet (pH 7.5). ChIP was performed using 2–10 μg of antibodies. For ChIP-seq, material from three to four mice was pooled prior to library generation.

ChIP-seq and Cistromic Analysis—ChIP DNA was prepared for sequencing according to the amplification protocol provided by Illumina. Deep sequencing was performed using Illumina Genome AnalyzerIIx, and sequencing reads were obtained using the Solexa analysis pipeline and mapped to the mouse genome (UCSC Genome Browser mm9) using Bowtie software (36). Peak calling was carried out by the HOMER software suite (37). Location analysis of ChIP-seq peaks was performed using the Cistrome platform (38). Rev-erbα ChIP-seq in liver and BAT are from GEO accession numbers GSE26345 (39) and GSE79167 (18), respectively. Rev-erbα ChIP-seq in EWAT is available under GEO accession number GSE79166. PPARγ ChIP-seq in 3T3-L1 is from GEO accession number GSE27450 (40), PPARγ ChIP-seq in EWAT is from GEO accession number GSE64458 (41), and PPARα ChIP-seq in liver is from accession number GSE61817 (42). Histone 3 lysine 27 acetylation ChIP-seq in EWAT is from GEO accession number GSE63964 (43).

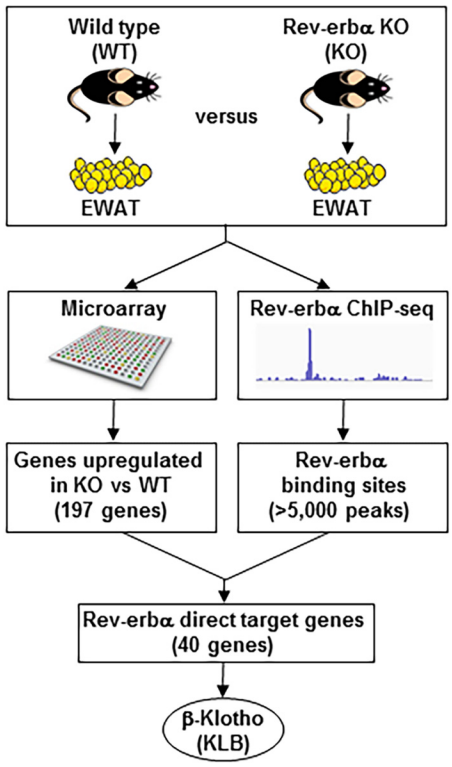

FIGURE 1. **Identification of *klb* as a direct target gene of Rev-erbα.** Rev-erbα direct target genes in EWAT were identified by combining Rev-erbα ChIP-seq data and a microarray performed on EWAT of WT and Rev-erbα KO mice at ZT 10 (5 p.m.). Of the direct target genes identified, *Klb* was the top candidate.

Global Run-on Sequencing (GRO-Seq)—The nuclear run-on assay was performed as described previously (44). GRO-seq reads were mapped to the mouse reference genome (mm9) and extended to 150-bp fragments. Gene body quantification was computed and normalized to reads per kb per ten million reads for each Refseq-annotated transcript. ChIP-seq and GRO-seq data were visualized using Integrative Genomics Viewer (IGV) (45). GRO-seq in 3T3-L1 adipocytes is from GEO accession number GSE56747 (46). GRO-seq performed on liver is from GEO accession number GSE59486 (44). GRO-seq performed on EWAT, IWAT, and BAT is available in GEO accession number GSE79168.

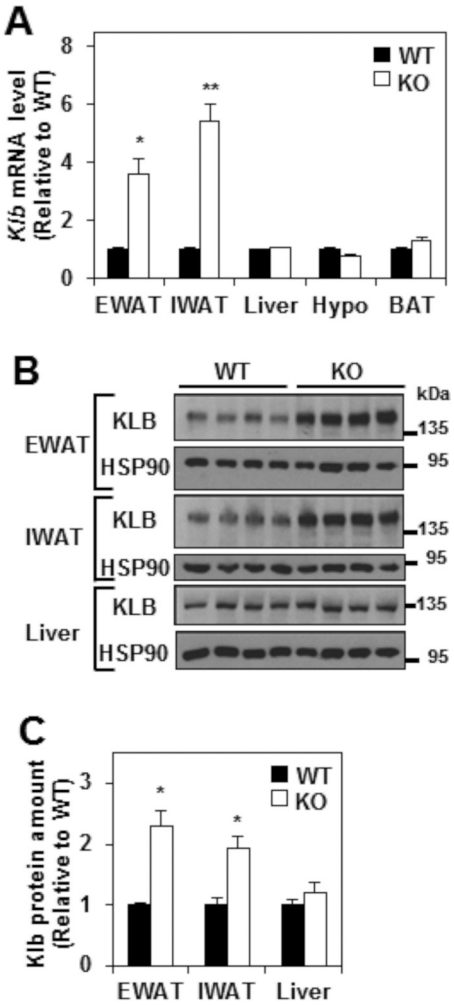

FIGURE 2. **βKlotho mRNA and protein levels are increased in white adipose tissue of Rev-erbα KO mice.** *A*, relative mRNA level of Klb in the EWAT, IWAT, liver, hypothalamus (*Hypo*), and BAT of WT and Rev-erbα KO mice at ZT 10. Data are expressed as the mean ± S.E. and normalized to the WT (Student's *t* test; *, $p < 0.01$; **, $p < 0.001$ *versus* WT; $n = 4–6$). *B* and *C*, Western blotting analysis of KLB and HSP90 (loading control) proteins levels in EWAT, IWAT, and liver of WT and Rev-erbα KO mice at ZT 10. Representative immunoblots are shown (*B*), and KLB protein amounts were quantified by densitometry scanning analysis, expressed as the mean ± S.E., normalized to the WT (Student's *t* test; *, $p < 0.01$ *versus* WT; $n = 4$).

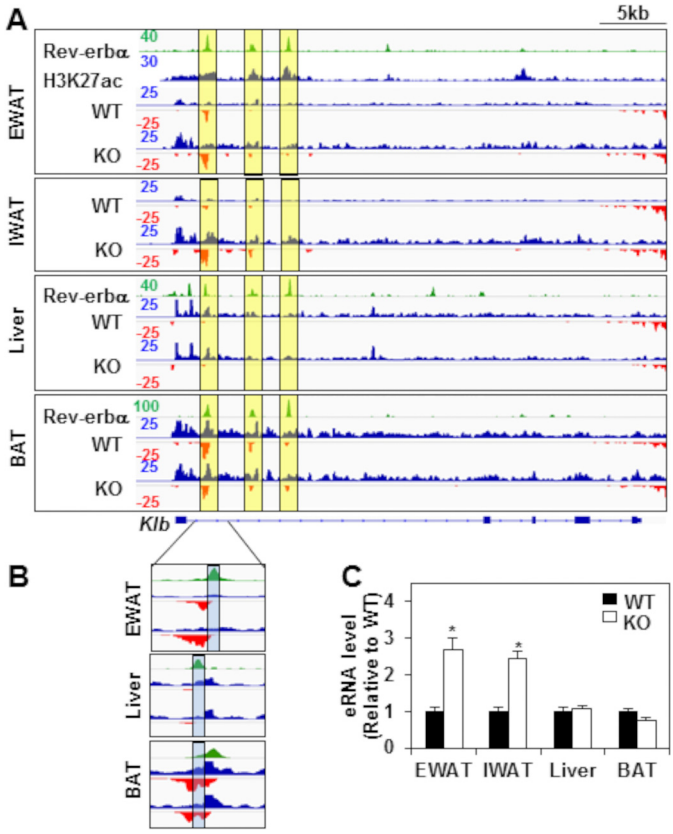

FIGURE 3. **Rev-erbα controls enhancer RNA expression at the *Klb* locus specifically in mouse white adipose tissue.** *A*, ChIP-seq profiles of Rev-erbα binding at the *Klb* locus (*green tracks*) in EWAT, liver (39), and BAT (18) of WT mice at ZT 10. Rev-erbα peaks at the *Klb* locus are highlighted in *yellow boxes*. Also shown are ChIP-seq profiles of H3K27ac at the *Klb* locus (*blue track*) in EWAT (43). GRO-seq was performed on EWAT, IWAT, liver, and BAT of WT and Rev-erbα KO mice at ZT 10. Genome browser views of nascent transcripts at the *Klb* locus are shown. GRO-seq signals on the + and − strand are illustrated in *blue* and *red*, respectively. Intragenic nascent eRNA at the *Klb* locus is highlighted in *yellow boxes*. The *y axis scale* refers to the normalized tag count per ten million reads. *B*, magnification of the major Rev-erbα peak at the *Klb* locus in EWAT, liver, and BAT. The center of eRNA in each tissue is highlighted in *blue*. *C*, RT-qPCR validation of transcription of intragenic eRNA at the *Klb* locus in EWAT, IWAT, liver, and BAT of WT and Rev-erbα KO mice. Tissues were harvested at ZT 10. Data are expressed as the mean ± S.E. and normalized to the WT (Student's *t* test; *, $p < 0.01$ *versus* WT; $n = 4$).

Statistics—Comparisons between two groups were performed using Student's *t* test. Multiple-group comparisons were performed by a two-way analysis of variance. Statistical significance was defined as $p < 0.05$. All data are presented as mean ± S.E.

Results

βKlotho (Klb) Is a Direct Target Gene of the Nuclear Receptor Rev-erbα in Adipose Tissue—To investigate the role of Rev-erbα in adipose tissue, epididymal WAT (EWAT) was collected from WT and Rev-erbα KO mice at ZT 10 (5 p.m.), when the Rev-erbα protein level peaks in WT mice, and subjected to microarray analysis of gene expression. Consistent with the transcriptional repression function of Rev-erbα, about twice as many genes were induced than decreased (with cut-off of -fold change >1.5 and $p < 0.01$) in Rev-erbα KO EWAT compared with the WT (Fig. 1). To identify induced genes that were direct targets of Rev-erbα, we performed chromatin immunoprecipitation using antibodies against Rev-erbα, followed by deep sequencing (ChIP-seq) of EWAT at ZT 10 (Fig. 1). More than 5000 Rev-erbα peaks were detected, and the integrated analysis of the genome-wide studies identified 40 genes up-regulated in the Rev-erbα KO EWAT microarray (with cut-off of -fold change >1.5 and $p < 0.01$) and with nearby Rev-erbα binding sites (with cut-off of binding strength >1.5 rpm). These 40 genes were considered to be potential direct target genes of Rev-erbα in EWAT. In this study we focused on *βKlotho* (*Klb*) because it was one of the most induced potential target genes of Rev-erbα in EWAT and is a critical regulator of FGF21 signaling and intermediate metabolism *in vitro* (28, 29) and *in vivo* (32, 47).

Klb mRNA and Protein Levels Are Increased in White Adipose Tissue of Rev-erbα KO Mice Compared with the WT—Consistent with our microarray result, the mRNA levels of *Klb* were robustly increased in both EWAT and inguinal WAT (IWAT)

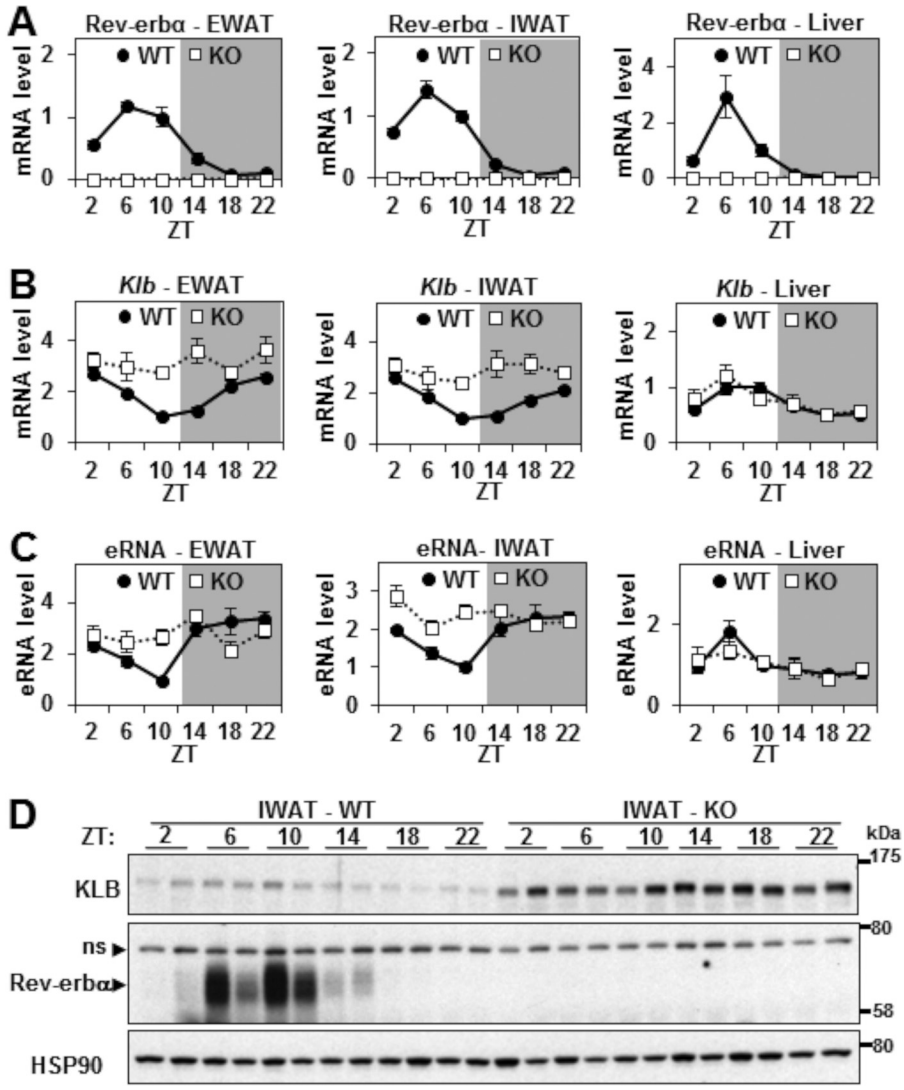

FIGURE 4. **Rev-erbα controls the circadian transcription of *Klb* in WAT.** *A* and *B*, relative mRNA levels of Rev-erbα (*A*) and *Klb* (*B*) in EWAT, IWAT, and liver of WT and Rev-erbα KO mice throughout 24 h. Values are the mean ± S.E. and normalized to the WT at ZT 10 ($n = 4–6$/time point). *C*, RT-qPCR of eRNA at the *Klb* locus in EWAT, IWAT, and liver of WT and Rev-erbα KO mice throughout 24 h. Data are expressed as the mean ± S.E. ($n = 4–6$/time point) and normalized to the WT at ZT 10. *D*, Western blotting analysis of KLB, Rev-erbα (*ns*, nonspecific band), and HSP90 (loading control) protein levels in IWAT of WT and Rev-erbα KO mice throughout 24 h ($n = 2$/time point). Representative immunoblots are presented.

of Rev-erbα KO mice compared with WT mice (Fig. 2*A*). In contrast, no significant change in *Klb* mRNA level was observed in liver, hypothalamus, and BAT (Fig. 2*A*). KLB protein levels were also markedly elevated in EWAT and IWAT, but not liver, of Rev-erbα KO mice (Fig. 2, *B* and *C*). These results suggest that Rev-erbα regulates the expression of *Klb* specifically in WAT.

Rev-erbα Controls Enhancer RNA Expression at the Klb locus Specifically in Mouse White Adipose Tissue—Inspection of the ChIP-seq data revealed three robust Rev-erbα binding sites within the first intron of the *Klb* locus in EWAT (48) but also in liver (39) and BAT (18) (Fig. 3*A*, *green tracks*, *yellow boxes*). To address the mechanism of the tissue-specific regulation of *Klb* transcription by Rev-erbα, we performed global run-on followed by high-throughput sequencing (GRO-seq) to measure nascent transcription in WAT, liver, and BAT of WT and Rev-erbα KO mice (Fig. 3*A*, the positive and negative strands are illustrated in *blue* and *red*, respectively). This revealed increased transcription of the *Klb* gene body in WAT, but not in BAT or liver, of Rev-erbα KO mice relative to the WT (Fig. 3*A*).

Because GRO-seq measures transcription wherever it occurs in the genome, it also detects bidirectional transcripts at enhancers, called eRNAs, whose regulation often correlates with that of nearby gene expression and is thus a useful measure of enhancer activity (49–51). Robust eRNA transcription was detected in the first intron of the *Klb* locus (Fig. 3*A*, *three yellow boxes*) and was greatest at the Rev-erbα binding site closest to the transcriptional start site (Fig. 3*A*, *left yellow boxes*). Indeed, the sites of strongest Rev-erbα binding were highly enriched for H3K27 acetylation in EWAT (Fig. 3*A*) (43), a well recognized epigenomic feature of active enhancers (52).

Changes in eRNA upon deletion of a transcription factor that binds at the enhancer can separate functional from non-functional binding sites (44). In this context, it is remarkable that deletion of Rev-erbα markedly increased the transcription of the most abundant eRNA in EWAT and IWAT (Fig. 3*A*, *left*

yellow boxes), whereas expression of the eRNA was constitutive in liver and BAT (Fig. 3*A*). When we zoomed in on the first peak, we found that it did not overlap in EWAT and liver (Fig. 3*B*, *blue boxes*). Indeed, the peaks were ~250 bp apart (Fig. 3*B*). Furthermore, the EWAT peak contained a DR2 motif and not the liver peak, explaining the different effects of Rev-erbα deletion on *Klb* transcription in EWAT and liver. In BAT, although Rev-erbα bound exactly the same site as in EWAT, that site was not at the center of the bidirectional eRNA locus (Fig. 3*B*, *blue boxes*), suggesting that it was not a part of the functional enhancer. The specific role of Rev-erbα at this enhancer in WATs was confirmed quantitatively by RT-qPCR in the different tissues of Rev-erbα KO mice compared with the WT (Fig. 3*C*). These results suggest that Rev-erbα is functionally active at this site in WAT but not BAT or liver, which would explain the tissue-specific regulation of *Klb* by Rev-erbα.

Rev-erbα Controls the Circadian Transcription of Klb in WAT—As expected, Rev-erbα expression was circadian, peaking at ZT 6–10 (1–5 p.m.), with a robust amplitude in the WAT and liver of WT mice (Fig. 4*A*). We hypothesized that Rev-erbα would repress the transcription of *Klb* in a circadian manner in WAT but not in liver. Indeed, *Klb* mRNA expression was circadian and antiphase to Rev-erbα in EWAT and IWAT, but not in liver, of WT mice (Fig. 4*B*). This circadian pattern was greatly attenuated in EWAT and IWAT of Rev-erbα KO mice (Fig. 4*B*) because of increased *Klb* expression at its normal nadir, indicating that Rev-erbα was responsible for the antiphase rhythm. RT-qPCR analysis demonstrated a similar Rev-erbα-dependent circadian rhythm of the eRNAs at the functional *Klb* enhancer in EWAT and IWAT, strongly suggesting direct transcriptional control of the circadian expression of *Klb* mRNA (Fig. 4*C*). Surprisingly, although the overall KLB protein expression was dramatically increased in Rev-erbα KO IWAT compared with the WT, the expression of KLB protein was not nearly as circadian as its mRNA, and the hint of a rhythm was not in synch with the mRNA (Fig. 4*D*), suggesting that post-transcriptional factors dampen the endogenous rhythm of KLB protein.

PPARγ Directly Modulates the Rev-erbα-regulated Enhancer at the Klb Locus—Given that Rev-erbα often binds to the genome near lineage determination factors (48), we hypothesized that the Rev-erbα-controlled enhancer might also be bound and modulated by PPARγ, the master regulator of adipocyte development and function (53–55). Indeed, PPARγ bound at the major Rev-erbα binding sites at the *Klb* locus in EWAT (41) (Fig. 5*A*, *purple track*). Interestingly, we found that PPARα bound at the major Rev-erbα binding sites at the *Klb* locus in liver (42) (Fig. 5*A*, *orange track*). Furthermore, we noted binding of PPARγ at the major Rev-erbα binding sites at the *Klb* locus in 3T3-L1 mouse adipocytes (40) (Fig. 5*B*). Moreover, analysis of GRO-seq in 3T3-L1 adipocytes (46) revealed that transcription at both the *Klb* gene body and the most transcription start site-proximal enhancer was increased as early as 10 min after addition of rosiglitazone (*rosi*), a potent synthetic agonist ligand of PPARγ (Fig. 5*C*). Moreover, *Klb* gene expression was down-regulated 14.6-fold after silencing PPARγ in 3T3-L1 adipocytes (35) (Fig. 5*D*), indicating that PPARγ was required for *Klb* transcription. These results show that PPARγ regulates the enhancer activity at the *Klb* locus in the opposite direction of Rev-erbα.

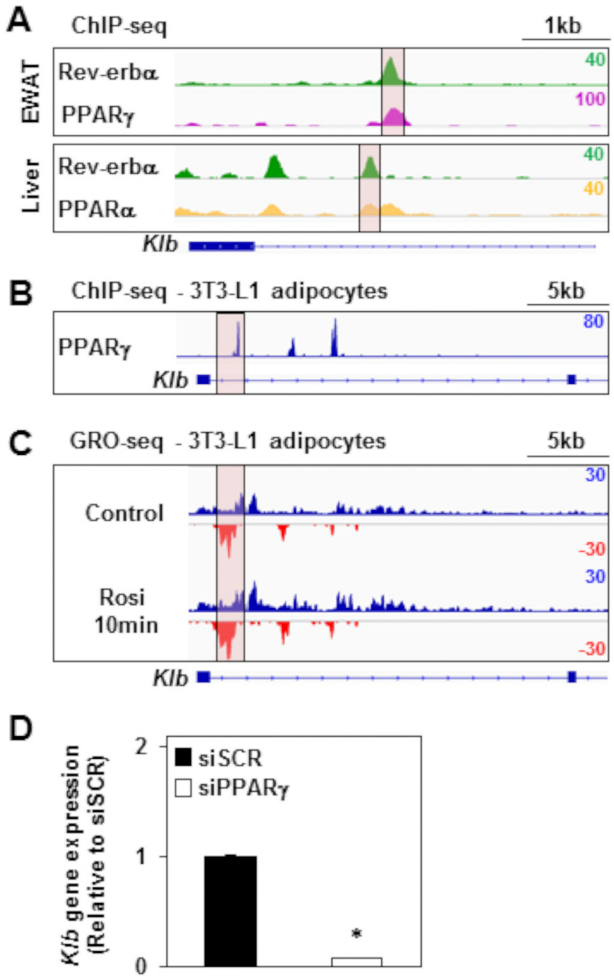

FIGURE 5. **PPARγ binds and modulates the Rev-erbα-regulated enhancer at the *Klb* locus.** *A*, ChIP-seq profiles of Rev-erbα (*green tracks*, also shown in Fig. 3*A*) (39, 48) and PPARγ (*purple track*) (41) or PPARα (*orange track*) (42) binding at the *Klb* locus in, respectively, EWAT or liver of WT mice. The major Rev-erbα peak at the *Klb* locus is highlighted in *pink*. The *y axis scale* refers to the normalized tag count per million reads. *B*, ChIP-seq profiles of PPARγ binding at the *Klb* locus in 3T3-L1 adipocytes (40). The *y axis scale* refers to the normalized tag count per million reads. *C*, GRO-seq was performed in 3T3-L1 adipocytes treated with rosiglitazone (*Rosi*) for 10 min or left untreated (46). Genome browser views of nascent transcripts at the *Klb* locus are shown. GRO-seq signals on the + and − strand are illustrated in *blue* and *red*, respectively. The *y axis scale* refers to the normalized tag count per million reads. *D*, *Klb* gene expression in 3T3-L1 adipocytes treated with siRNA against scrambled (*siSCR*) or PPARγ (*siPPARγ*) mRNA (35). Data are expressed as the mean ± S.E. and normalized to the WT (Student's *t* test; *, $p < 0.001$ *versus* the WT; $n = 3$).

FGF21 Action Is Enhanced in WAT of Rev-erbα KO Mice—Previous work has demonstrated that KLB is essential for FGF21 activity both *in vitro* (28, 29) and *in vivo* (32, 47) and that KLB in adipose tissue contributes to the beneficial metabolic actions of FGF21 (32). Therefore, we tested whether the up-regulation of KLB in the WAT of Rev-erbα KO mice sensitized the mice to the effect of FGF21 by treating WT and Rev-erbα KO mice with either vehicle or recombinant human FGF21 protein and then measuring the expression of FGF21 target genes in WAT. As expected, FGF21 significantly induced the EWAT expression of *cFos*, *Egr1*, and *Glut1* (by 2.1-, 14.4-, and 1.7-fold, respectively) in WT mice (Fig. 6, *A*–*C*). However, the

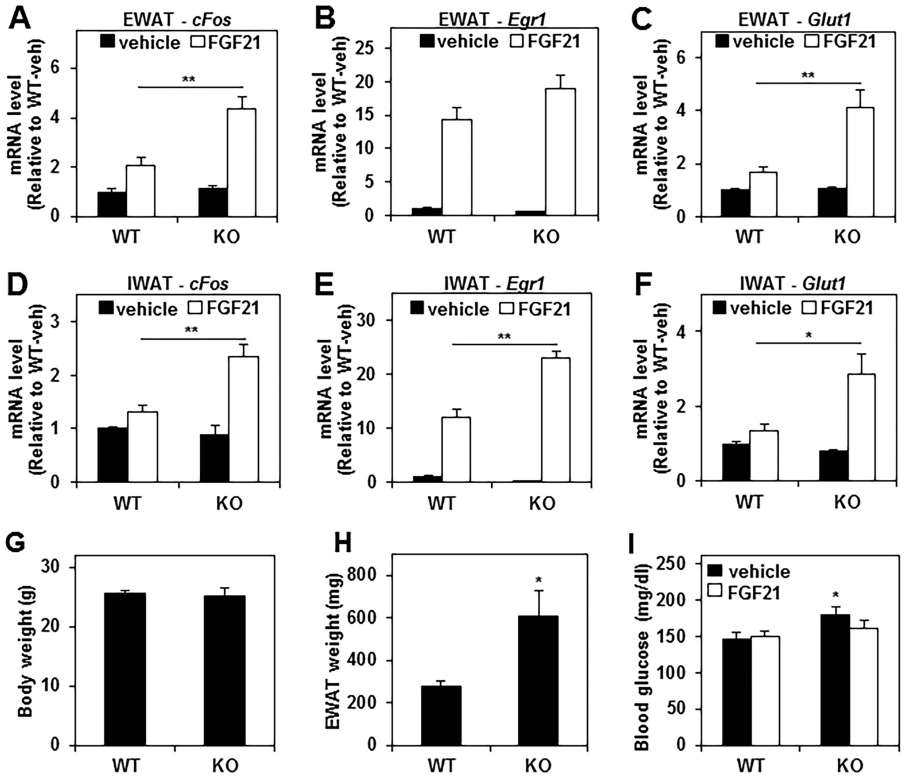

FIGURE 6. **The FGF21 response is enhanced in white adipose tissue of Rev-erbα KO mice.** *A–F*, relative mRNA levels of the FGF21 target genes *cFos*, *Egr1*, and *Glut1* in EWAT (*A–C*) and IWAT (*D--F*) of WT and Rev-erbα KO mice injected with either vehicle or 0.6 mg/kg FGF21. Tissues were harvested at ZT 10, 2 h after the injection. Values are expressed as the mean ± S.E. and normalized to WT vehicle (two-way analysis of variance and Tukey's post hoc test; *, $p < 0.01$; **, $p < 0.001$; $n = 8$). *G* and *H*, body weight (*G*) and EWAT weight (*H*) of WT and Rev-erbα KO mice. Data are expressed as the mean ± S.E. (Student's *t* test; *, $p < 0.05$ *versus* WT; $n = 5$). *I*, blood glucose level of WT and Rev-erbα KO mice injected with either vehicle or 0.6 mg/kg of FGF21. Blood was collected at ZT 10, 2 h after the injection. Data are expressed as the mean ± S.E. (two-way analysis of variance; *, $p < 0.05$ *versus* WT vehicle; $n = 6$).

induction of these three genes by FGF21 treatment was much more dramatic in Rev-erbα KO mice (3.9-fold for cFos, 34.8-fold for Egr1, and 4-fold for Glut1) (Fig. 6, *A–C*). Similarly, a more robust FGF21 response was also observed in IWAT of Rev-erbα KO mice compared with WT mice (Fig. 6, *D–F*). As described previously, mice lacking Rev-erbα displayed a similar body weight (Fig. 6*G*) and increased adiposity (Fig. 6*H*) compared with wild-type mice on a chow diet (56). Moreover, Rev-erbα KO mice exhibited mild hyperglycemia without insulin resistance compared with wild-type mice on a chow diet (56). Of note, the modest hyperglycemia exhibited by Rev-erbα KO mice (Fig. 6*I*) was abrogated by FGF21 treatment (Fig. 6*I*). Together, these results indicate that Rev-erbα plays an important role in restraining FGF21 signaling in WAT, most likely through the direct repression of its co-receptor, KLB.

Discussion

We have demonstrated that the deletion of Rev-erbα leads to the up-regulation of βKlotho, an essential co-receptor for FGF21, specifically in WAT, where it modulates the downstream effects of the FGF21 pathway. These findings reveal an important and previously unrecognized role for Rev-erbα in adipose function.

Rev-erbα bound to the *Klb* locus in different metabolic tissues, including WAT, BAT, and liver, but the induction of *Klb* transcription upon Rev-erbα deletion was restricted to WAT. This is consistent with previous findings that Rev-erbα is not transcriptionally active at all of its cistromic binding sites in the liver (44, 48). The Rev-erbα dependence of eRNA transcription in WAT but not in other tissues may not only reflect the activity of the *Klb* enhancers but could also be playing a direct role in transcriptional regulation, as reported in macrophages (57).

Some tissue-specific functions of Rev-erbα are explained by its selective binding near lineage determination factors such as hepatocyte nuclear factor 6 (HNF6) in liver (48). In this context, it is noteworthy that we found the Rev-erbα binding regions of the *Klb* locus to also be occupied by the nuclear receptor PPARγ, the master lineage determination factor for adipose tissue (53–55). Ligand activation of PPARγ acted in the opposite direction, inducing the transcription of *Klb* and its eRNAs. KLB was also found to be up-regulated in EWAT of mice treated with PPARγ ligands (58, 59). Moreover, knockdown of PPARγ led to a decrease in KLB mRNA level in 3T3-L1 adipocytes. However, PPARγ is not likely to be specifically required for Rev-erbα binding in WAT because we observed comparable binding in liver, which expresses very low levels of PPARγ. Therefore it is likely that WAT-specific coregulator recruitment or chromatin remodeling plays a role in the tissue specificity of Rev-erbα regulation of *Klb.*

Previous studies have identified a clear link between the molecular clock and hepatic FGF21 signaling (60, 61), including suppression of *Fgf21* transcription by E4BP4, which is a direct Rev-erbα target in liver (60). In addition, Rev-erbα has been

shown to modulate FGF21 expression in liver (62). Given the circadian expression of Rev-erbα in WAT, we hypothesized that the repression by Rev-erbα would also be rhythmic. Indeed, we demonstrated circadian mRNA expression of *Klb* and its enhancer activity in WAT, and this was antiphase to, and dependent upon, the expression of Rev-erbα. Surprisingly, although KLB protein levels were dramatically elevated at all times of day in Rev-erbα KO WAT compared with the WT, its normal protein expression was hardly, if at all, circadian and did not follow the pattern of circadian *Klb* gene expression of the *Klb* mRNA. This phenomenon may be caused by posttranscriptional mechanisms and suggests that KLB protein has a long half-life that reduces the impact of circadian gene expression on KLB protein levels. The physiological significance of the robust, Rev-erbα-dependent circadian rhythm of *Klb* gene expression is thus unclear. It is possible that the *Klb* mRNA half-life is regulated so that the Rev-erbα-driven rhythm becomes significant in some physiological states, but this has yet to be shown. Because KLB protein levels were not found to be normally circadian but were markedly and constitutively elevated in WAT of Rev-erbα KO mice, we focused mainly on the effects of FGF21 in this system.

The beneficial effects of FGF21 on glucose metabolism and body weight have identified it as a central player in regulating metabolic processes, and adipose tissue is required for its antidiabetic actions (32, 33, 63). These findings show that FGF21 signaling is modulated by Rev-erbα in WAT, not by altering FGF21 levels but through the regulation of its co-receptor KLB in WAT but not in liver. Consistent with this, FGF21 target genes, including early response genes and GLUT1, were superinduced in WAT after treatment of Rev-erbα KO mice with recombinant FGF21. Moreover, FGF21 had a modest effect on glycemia in Rev-erbα KO mice. It is tempting to speculate that this is related to the increase in GLUT1 expression, but there are many other potential mechanisms, including systemic effects of FGF21, beyond its direct actions on WAT.

In summary, this study extends our knowledge about Rev-erbα functions in mouse adipose tissue and provides further sights into the mechanisms underlying the FGF21 actions in fat. The development of appropriate synthetic Rev-erbα antagonists could be beneficial in facilitating FGF21-related therapeutic approaches for various metabolic diseases.

Author Contributions—J. J., F. W., and M. A. L. conceived the project design and wrote the manuscript. J. J., F. W., L. C. P., and D. J. S. gathered the data. J. J., F. W., B. F., H. W. L., K. J. W., and M. A. L. analyzed the data. A. K. and A. C. A. provided the recombinant FGF21 and comments and suggestions for improvement of the manuscript.

Acknowledgments—We thank the Functional Genomics Core (J. Schug and K. Kaestner) of the Penn Diabetes Research Center (P30 DK19525) for next-generation sequencing. We also thank the Penn Microarray Core for microarray analysis.

References

1. Qatanani, M., and Lazar, M. A. (2007) Mechanisms of obesity-associated insulin resistance: many choices on the menu. *Genes Dev.* **21,** 1443–1455
2. Anghel, S. I., and Wahli, W. (2007) Fat poetry: a kingdom for PPAR γ. *Cell Res.* **17,** 486–511
3. Guilherme, A., Virbasius, J. V., Puri, V., and Czech, M. P. (2008) Adipocyte dysfunctions linking obesity to insulin resistance and type 2 diabetes. *Nat. Rev. Mol. Cell Biol.* **9,** 367–377
4. Mathieu, P., Lemieux, I., and Després, J. P. (2010) Obesity, inflammation, and cardiovascular risk. *Clin. Pharmacol. Ther.* **87,** 407–416
5. Ouchi, N., Parker, J. L., Lugus, J. J., and Walsh, K. (2011) Adipokines in inflammation and metabolic disease. *Nat. Rev. Immunol.* **11,** 85–97
6. Gronemeyer, H., Gustafsson, J. A., and Laudet, V. (2004) Principles for modulation of the nuclear receptor superfamily. *Nat. Rev. Drug. Discov.* **3,** 950–964
7. Mangelsdorf, D. J., Thummel, C., Beato, M., Herrlich, P., Schütz, G., Umesono, K., Blumberg, B., Kastner, P., Mark, M., Chambon, P., and Evans, R. M. (1995) The nuclear receptor superfamily: the second decade. *Cell* **83,** 835–839
8. Yang, X., Lamia, K. A., and Evans, R. M. (2007) Nuclear receptors, metabolism, and the circadian clock. *Cold Spring Harbor Symp. Quant. Biol.* **72,** 387–394
9. Harding, H. P., and Lazar, M. A. (1995) The monomer-binding orphan receptor Rev-Erb represses transcription as a dimer on a novel direct repeat. *Mol. Cell. Biol.* **15,** 4791–4802
10. Ishizuka, T., and Lazar, M. A. (2003) The N-CoR/histone deacetylase 3 complex is required for repression by thyroid hormone receptor. *Mol. Cell. Biol.* **23,** 5122–5131
11. Zamir, I., Harding, H. P., Atkins, G. B., Hörlein, A., Glass, C. K., Rosenfeld, M. G., and Lazar, M. A. (1996) A nuclear hormone receptor corepressor mediates transcriptional silencing by receptors with distinct repression domains. *Mol. Cell. Biol.* **16,** 5458–5465
12. Preitner, N., Damiola, F., Lopez-Molina, L., Zakany, J., Duboule, D., Albrecht, U., and Schibler, U. (2002) The orphan nuclear receptor REV-ERBα controls circadian transcription within the positive limb of the mammalian circadian oscillator. *Cell* **110,** 251–260
13. Bugge, A., Feng, D., Everett, L. J., Briggs, E. R., Mullican, S. E., Wang, F., Jager, J., and Lazar, M. A. (2012) Rev-erbα and Rev-erbβ coordinately protect the circadian clock and normal metabolic function. *Genes Dev.* **26,** 657–667
14. Duez, H., and Staels, B. (2010) Nuclear receptors linking circadian rhythms and cardiometabolic control. *Arterioscler. Thromb. Vasc. Biol.* **30,** 1529–1534
15. Le Martelot, G., Claudel, T., Gatfield, D., Schaad, O., Kornmann, B., Lo Sasso, G., Moschetta, A., and Schibler, U. (2009) REV-ERBα participates in circadian SREBP signaling and bile acid homeostasis. *PLoS Biol.* **7,** e1000181
16. Gibbs, J. E., Blaikley, J., Beesley, S., Matthews, L., Simpson, K. D., Boyce, S. H., Farrow, S. N., Else, K. J., Singh, D., Ray, D. W., and Loudon, A. S. (2012) The nuclear receptor REV-ERBα mediates circadian regulation of innate immunity through selective regulation of inflammatory cytokines. *Proc. Natl. Acad. Sci. U.S.A.* **109,** 582–587
17. Woldt, E., Sebti, Y., Solt, L. A., Duhem, C., Lancel, S., Eeckhoute, J., Hesselink, M. K., Paquet, C., Delhaye, S., Shin, Y., Kamenecka, T. M., Schaart, G., Lefebvre, P., Nevière, R., Burris, T. P., Schrauwen, P., Staels, B., and Duez, H. (2013) Rev-erb-α modulates skeletal muscle oxidative capacity by regulating mitochondrial biogenesis and autophagy. *Nat. Med.* **19,** 1039–1046
18. Gerhart-Hines, Z., Feng, D., Emmett, M. J., Everett, L. J., Loro, E., Briggs, E. R., Bugge, A., Hou, C., Ferrara, C., Seale, P., Pryma, D. A., Khurana, T. S., and Lazar, M. A. (2013) The nuclear receptor Rev-erbα controls circadian thermogenic plasticity. *Nature* **503,** 410–413
19. Jager, J., O'Brien, W. T., Manlove, J., Krizman, E. N., Fang, B., Gerhart-Hines, Z., Robinson, M. B., Klein, P. S., and Lazar, M. A. (2014) Behavioral changes and dopaminergic dysregulation in mice lacking the nuclear receptor Rev-erbα. *Mol. Endocrinol.* **28,** 490–498
20. Potthoff, M. J., Kliewer, S. A., and Mangelsdorf, D. J. (2012) Endocrine fibroblast growth factors 15/19 and 21: from feast to famine. *Genes Dev.* **26,** 312–324
21. Kharitonenkov, A., and Adams, A. C. (2014) Inventing new medicines: the FGF21 story. *Mol. Metab.* **3,** 221–229

22. Kharitonenkov, A., Shiyanova, T. L., Koester, A., Ford, A. M., Micanovic, R., Galbreath, E. J., Sandusky, G. E., Hammond, L. J., Moyers, J. S., Owens, R. A., Gromada, J., Brozinick, J. T., Hawkins, E. D., Wroblewski, V. J., Li, D. S., Mehrbod, F., Jaskunas, S. R., and Shanafelt, A. B. (2005) FGF-21 as a novel metabolic regulator. *J. Clin. Invest.* **115,** 1627–1635
23. Coskun, T., Bina, H. A., Schneider, M. A., Dunbar, J. D., Hu, C. C., Chen, Y., Moller, D. E., and Kharitonenkov, A. (2008) Fibroblast growth factor 21 corrects obesity in mice. *Endocrinology* **149,** 6018–6027
24. Kharitonenkov, A., Wroblewski, V. J., Koester, A., Chen, Y. F., Clutinger, C. K., Tigno, X. T., Hansen, B. C., Shanafelt, A. B., and Etgen, G. J. (2007) The metabolic state of diabetic monkeys is regulated by fibroblast growth factor-21. *Endocrinology* **148,** 774–781
25. Wente, W., Efanov, A. M., Brenner, M., Kharitonenkov, A., Köster, A., Sandusky, G. E., Sewing, S., Treinies, I., Zitzer, H., and Gromada, J. (2006) Fibroblast growth factor-21 improves pancreatic β-cell function and survival by activation of extracellular signal-regulated kinase 1/2 and Akt signaling pathways. *Diabetes* **55,** 2470–2478
26. Berglund, E. D., Li, C. Y., Bina, H. A., Lynes, S. E., Michael, M. D., Shanafelt, A. B., Kharitonenkov, A., and Wasserman, D. H. (2009) Fibroblast growth factor 21 controls glycemia via regulation of hepatic glucose flux and insulin sensitivity. *Endocrinology* **150,** 4084–4093
27. Fisher, F. M., Kleiner, S., Douris, N., Fox, E. C., Mepani, R. J., Verdeguer, F., Wu, J., Kharitonenkov, A., Flier, J. S., Maratos-Flier, E., and Spiegelman, B. M. (2012) FGF21 regulates PGC-1alpha and browning of white adipose tissues in adaptive thermogenesis. *Genes Dev.* **26,** 271–281
28. Kharitonenkov, A., Dunbar, J. D., Bina, H. A., Bright, S., Moyers, J. S., Zhang, C., Ding, L., Micanovic, R., Mehrbod, S. F., Knierman, M. D., Hale, J. E., Coskun, T., and Shanafelt, A. B. (2008) FGF-21/FGF-21 receptor interaction and activation is determined by βKlotho. *J. Cell. Physiol.* **215,** 1–7
29. Ogawa, Y., Kurosu, H., Yamamoto, M., Nandi, A., Rosenblatt, K. P., Goetz, R., Eliseenkova, A. V., Mohammadi, M., and Kuro-o, M. (2007) βKlotho is required for metabolic activity of fibroblast growth factor 21. *Proc. Natl. Acad. Sci. U.S.A.* **104,** 7432–7437
30. Suzuki, M., Uehara, Y., Motomura-Matsuzaka, K., Oki, J., Koyama, Y., Kimura, M., Asada, M., Komi-Kuramochi, A., Oka, S., and Imamura, T. (2008) βKlotho is required for fibroblast growth factor (FGF) 21 signaling through FGF receptor (FGFR) 1c and FGFR3c. *Mol. Endocrinol.* **22,** 1006–1014
31. Fon Tacer, K., Bookout, A. L., Ding, X., Kurosu, H., John, G. B., Wang, L., Goetz, R., Mohammadi, M., Kuro-o, M., Mangelsdorf, D. J., and Kliewer, S. A. (2010) Research resource: comprehensive expression atlas of the fibroblast growth factor system in adult mouse. *Mol. Endocrinol.* **24,** 2050–2064
32. Ding, X., Boney-Montoya, J., Owen, B. M., Bookout, A. L., Coate, K. C., Mangelsdorf, D. J., and Kliewer, S. A. (2012) βKlotho is required for fibroblast growth factor 21 effects on growth and metabolism. *Cell Metab.* **16,** 387–393
33. Adams, A. C., Yang, C., Coskun, T., Cheng, C. C., Gimeno, R. E., Luo, Y., and Kharitonenkov, A. (2012) The breadth of FGF21's metabolic actions are governed by FGFR1 in adipose tissue. *Mol. Metab.* **2,** 31–37
34. Wu, A. L., Kolumam, G., Stawicki, S., Chen, Y., Li, J., Zavala-Solorio, J., Phamluong, K., Feng, B., Li, L., Marsters, S., Kates, L., van Bruggen, N., Leabman, M., Wong, A., West, D., Stern, H., Luis, E., Kim, H. S., Yansura, D., Peterson, A. S., Filvaroff, E., Wu, Y., and Sonoda, J. (2011) Amelioration of type 2 diabetes by antibody-mediated activation of fibroblast growth factor receptor 1. *Sci. Transl. Med.* **3,** 113ra126
35. Schupp, M., Cristancho, A. G., Lefterova, M. I., Hanniman, E. A., Briggs, E. R., Steger, D. J., Qatanani, M., Curtin, J. C., Schug, J., Ochsner, S. A., McKenna, N. J., and Lazar, M. A. (2009) Re-expression of GATA2 cooperates with peroxisome proliferator-activated receptor-γ depletion to revert the adipocyte phenotype. *J. Biol. Chem.* **284,** 9458–9464
36. Langmead, B., Trapnell, C., Pop, M., and Salzberg, S. L. (2009) Ultrafast and memory-efficient alignment of short DNA sequences to the human genome. *Genome Biol.* **10,** R25
37. Heinz, S., Benner, C., Spann, N., Bertolino, E., Lin, Y. C., Laslo, P., Cheng, J. X., Murre, C., Singh, H., and Glass, C. K. (2010) Simple combinations of lineage-determining transcription factors prime cis-regulatory elements required for macrophage and B cell identities. *Mol. Cell* **38,** 576–589
38. Liu, T., Ortiz, J. A., Taing, L., Meyer, C. A., Lee, B., Zhang, Y., Shin, H., Wong, S. S., Ma, J., Lei, Y., Pape, U. J., Poidinger, M., Chen, Y., Yeung, K., Brown, M., Turpaz, Y., and Liu, X. S. (2011) Cistrome: an integrative platform for transcriptional regulation studies. *Genome Biol.* **12,** R83
39. Feng, D., Liu, T., Sun, Z., Bugge, A., Mullican, S. E., Alenghat, T., Liu, X. S., and Lazar, M. A. (2011) A circadian rhythm orchestrated by histone deacetylase 3 controls hepatic lipid metabolism. *Science* **331,** 1315–1319
40. Schmidt, S. F., Jørgensen, M., Chen, Y., Nielsen, R., Sandelin, A., and Mandrup, S. (2011) Cross species comparison of C/EBPα and PPARγ profiles in mouse and human adipocytes reveals interdependent retention of binding sites. *BMC Genomics* **12,** 152
41. Soccio, R. E., Chen, E. R., Rajapurkar, S. R., Safabakhsh, P., Marinis, J. M., Dispirito, J. R., Emmett, M. J., Briggs, E. R., Fang, B., Everett, L. J., Lim, H. W., Won, K. J., Steger, D. J., Wu, Y., Civelek, M., Voight, B. F., and Lazar, M. A. (2015) Genetic variation determines PPARγ function and anti-diabetic drug response *in vivo*. *Cell* **162,** 33–44
42. Lee, J. M., Wagner, M., Xiao, R., Kim, K. H., Feng, D., Lazar, M. A., and Moore, D. D. (2014) Nutrient-sensing nuclear receptors coordinate autophagy. *Nature* **516,** 112–115
43. Harms, M. J., Lim, H. W., Ho, Y., Shapira, S. N., Ishibashi, J., Rajakumari, S., Steger, D. J., Lazar, M. A., Won, K. J., and Seale, P. (2015) PRDM16 binds MED1 and controls chromatin architecture to determine a brown fat transcriptional program. *Genes Dev.* **29,** 298–307
44. Fang, B., Everett, L. J., Jager, J., Briggs, E., Armour, S. M., Feng, D., Roy, A., Gerhart-Hines, Z., Sun, Z., and Lazar, M. A. (2014) Circadian enhancers coordinate multiple phases of rhythmic gene transcription *in vivo*. *Cell* **159,** 1140–1152
45. Robinson, J. T., Thorvaldsdóttir, H., Winckler, W., Guttman, M., Lander, E. S., Getz, G., and Mesirov, J. P. (2011) Integrative genomics viewer. *Nat. Biotechnol.* **29,** 24–26
46. Step, S. E., Lim, H. W., Marinis, J. M., Prokesch, A., Steger, D. J., You, S. H., Won, K. J., and Lazar, M. A. (2014) Anti-diabetic rosiglitazone remodels the adipocyte transcriptome by redistributing transcription to PPARγ-driven enhancers. *Genes Dev.* **28,** 1018–1028
47. Adams, A. C., Cheng, C. C., Coskun, T., and Kharitonenkov, A. (2012) FGF21 requires βklotho to act *in vivo*. *PLoS ONE* **7,** e49977
48. Zhang, Y., Fang, B., Emmett, M. J., Damle, M., Sun, Z., Feng, D., Armour, S. M., Remsberg, J. R., Jager, J., Soccio, R. E., Steger, D. J., and Lazar, M. A. (2015) Gene regulation: discrete functions of nuclear receptor Rev-erbα couple metabolism to the clock. *Science* **348,** 1488–1492
49. Core, L. J., Waterfall, J. J., and Lis, J. T. (2008) Nascent RNA sequencing reveals widespread pausing and divergent initiation at human promoters. *Science* **322,** 1845–1848
50. Hah, N., Murakami, S., Nagari, A., Danko, C. G., and Kraus, W. L. (2013) Enhancer transcripts mark active estrogen receptor binding sites. *Genome Res.* **23,** 1210–1223
51. Kim, T. K., Hemberg, M., Gray, J. M., Costa, A. M., Bear, D. M., Wu, J., Harmin, D. A., Laptewicz, M., Barbara-Haley, K., Kuersten, S., Markenscoff-Papadimitriou, E., Kuhl, D., Bito, H., Worley, P. F., Kreiman, G., and Greenberg, M. E. (2010) Widespread transcription at neuronal activity-regulated enhancers. *Nature* **465,** 182–187
52. Creyghton, M. P., Cheng, A. W., Welstead, G. G., Kooistra, T., Carey, B. W., Steine, E. J., Hanna, J., Lodato, M. A., Frampton, G. M., Sharp, P. A., Boyer, L. A., Young, R. A., and Jaenisch, R. (2010) Histone H3K27ac separates active from poised enhancers and predicts developmental state. *Proc. Natl. Acad. Sci. U.S.A.* **107,** 21931–21936
53. Chawla, A., Schwarz, E. J., Dimaculangan, D. D., and Lazar, M. A. (1994) Peroxisome proliferator-activated receptor (PPAR) γ: adipose-predominant expression and induction early in adipocyte differentiation. *Endocrinology* **135,** 798–800
54. Tontonoz, P., Hu, E., Graves, R. A., Budavari, A. I., and Spiegelman, B. M. (1994) mPPAR γ 2: tissue-specific regulator of an adipocyte enhancer. *Genes Dev.* **8,** 1224–1234
55. Tontonoz, P., Hu, E., and Spiegelman, B. M. (1994) Stimulation of adipogenesis in fibroblasts by PPAR γ 2, a lipid-activated transcription factor. *Cell* **79,** 1147–1156
56. Delezie, J., Dumont, S., Dardente, H., Oudart, H., Gréchez-Cassiau, A.,

Klosen, P., Teboul, M., Delaunay, F., Pévet, P., and Challet, E. (2012) The nuclear receptor REV-ERBα is required for the daily balance of carbohydrate and lipid metabolism. *FASEB J.* **26,** 3321–3335

57. Lam, M. T., Cho, H., Lesch, H. P., Gosselin, D., Heinz, S., Tanaka-Oishi, Y., Benner, C., Kaikkonen, M. U., Kim, A. S., Kosaka, M., Lee, C. Y., Watt, A., Grossman, T. R., Rosenfeld, M. G., Evans, R. M., and Glass, C. K. (2013) Rev-Erbs repress macrophage gene expression by inhibiting enhancer-directed transcription. *Nature* **498,** 511–515
58. Adams, A. C., Coskun, T., Cheng, C. C., O'Farrell, L. S., Dubois, S. L., and Kharitonenkov, A. (2013) Fibroblast growth factor 21 is not required for the antidiabetic actions of the thiazoladinediones. *Mol. Metab.* **2,** 205–214
59. Moyers, J. S., Shiyanova, T. L., Mehrbod, F., Dunbar, J. D., Noblitt, T. W., Otto, K. A., Reifel-Miller, A., and Kharitonenkov, A. (2007) Molecular determinants of FGF-21 activity-synergy and cross-talk with PPARγ signaling. *J. Cell. Physiol.* **210,** 1–6
60. Tong, X., Muchnik, M., Chen, Z., Patel, M., Wu, N., Joshi, S., Rui, L., Lazar, M. A., and Yin, L. (2010) Transcriptional repressor E4-binding protein 4 (E4BP4) regulates metabolic hormone fibroblast growth factor 21 (FGF21) during circadian cycles and feeding. *J. Biol. Chem.* **285,** 36401–36409
61. Wang, Y., Solt, L. A., and Burris, T. P. (2010) Regulation of FGF21 expression and secretion by retinoic acid receptor-related orphan receptor α. *J. Biol. Chem.* **285,** 15668–15673
62. Estall, J. L., Ruas, J. L., Choi, C. S., Laznik, D., Badman, M., Maratos-Flier, E., Shulman, G. I., and Spiegelman, B. M. (2009) PGC-1α negatively regulates hepatic FGF21 expression by modulating the heme/Rev-Erbα axis. *Proc. Natl. Acad. Sci. U.S.A.* **106,** 22510–22515
63. Véniant, M. M., Hale, C., Helmering, J., Chen, M. M., Stanislaus, S., Busby, J., Vonderfecht, S., Xu, J., and Lloyd, D. J. (2012) FGF21 promotes metabolic homeostasis via white adipose and leptin in mice. *PLoS ONE* **7,** e40164